DJS Vol. 44 (1) (2022) pp. 123- 134 - ISSN: 1012-5965

ACCREDITED 2016
1969

Delta Journal of Science

Available online at **https://djs.journals.ekb.eg/**

Research Article

GEOLOGY

Integration of 3D seismic attributes and production history in revaluation of gas potential - Abu Madi and El Qaraa fields

Adel Othman[1], Mohamed Fathy[1], Justin Matresu[2], Mohamed Nassar[3]

1 Al-Azhar University, Nasr City, Cairo, Egypt
2 Eni International
3 Belayim Petroleum Company (Petrobel), Nasr City, Cairo, Egypt

Corresponding author: Mohamed Nassar **e-mail:**geo3nassar@gmail.com

Received: 13/1/2022 **accepted: 8/3/2022**

KEY WORDS

seismic attributes, Abu Madi, El Qaraa, post stack inversion

ABSTRACT

Using seismic AVO attributes and Inversion methods in predicting reservoir properties and geometry is an effective technique, especially in the Nile delta where the reservoir is heterogeneous. The main challenge in the current study is that most of the wells drilled in the area are either depleted or water folded. So the identification of gas-bearing sand using only seismic methods will be questionable. One of the advantages of the brownfield is that a lot of pertophysical data and production data are available.

Petrophysical data and production history help to understand the reservoir properties like porosity, density, shale content, fluid content, and water level (gas water contact GWC).

This study focused on using petrophysical and production data with the seismic inversion result to define the gas sand distribution and reservoir properties.

To achieve the target of the study Structural interpretation, amplitude, p-impedance, and VP/VS maps were created to improve imaging of Abu Madi reservoir levels. The production history of the closed & current production wells has been revised and integrated with the seismic results. Based on these new information areas of possible residual gas were delineated.

1. Introduction

The present Nile Delta is known as Neogene–Quaternary Delta. The Fayum Delta (Upper Eocene–Oligocene) and Moghra Delta (Early Miocene) are the ancestries of the present Nile Delta. The Fayum Delta and Moghra represent deposits of the ancestral Nile, which flowed in a northwesterly direction across the present-day El Bahr depression into the Mediterranean Sea **(Said *et al*., 1962)**. After that, an eastward shift of the Nile and its delta took place during Early to Middle Miocene time forming the present Nile Delta (Neogene–Quaternary Nile Delta). The shifting of the river from west to east may be a result of tilting and crustal movements that affected northern Egypt **(Salem *et al*., 1976)**.

The Abu Madi- El Qaraa (AM-EQ) Field is located onshore north of the Nile Delta, Egypt, Fig. (1). IEOC Company, considered the first gas discovery in Nile Delta, discovered it in 1967. The production began in 1975, is considered a giant gas and condensate accumulation for that time.

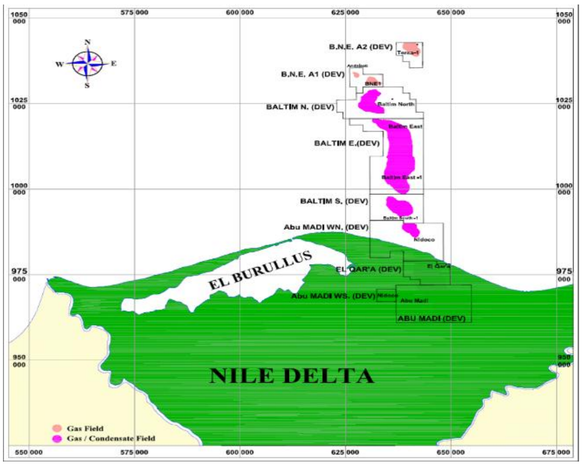

Fig. 1: Location map of Abu Madi - El Qaraa Field, northern Nile Delta Basin.

The field comprises two separate gas pools (termed Levels II and III) Fig. (3) within the Upper Miocene (Late Messinian) Abu Madi Formation, **(Barbieri *et al*., 1992)**. Level III has been penetrated by 19 wells. In 2014 only one well was still in production, the other 18 well have been water flooded. In 2002 the geometry and extension of Level III has been studied using the available 2D lines and wells data this study considered all level III comprises two main channel deposits, with subsidiary channel sands and, in the northeast, an alluvial-fan body Fig. (2) in hydrodynamic communication and has the same GWC with the presence of transmissibility which caused differential GWC rise.

Most reservoir study conducted for Abu Madi/El Qaraa fields done in 2002, formerly of the first 3D seismic acquisition and processing 2007-2008. Therefore, most of these studies accomplished for Abu Madi reservoirs (Level III and Level II) did not beneficiated the input of new 3D seismic data Fig. (2).

In the current work the new 3D seismic data, production data, and electrical logs data were integrated to update the maps, confirm reservoir geometry and continuity, also highlight new drilling opportunities for additional potential resources.

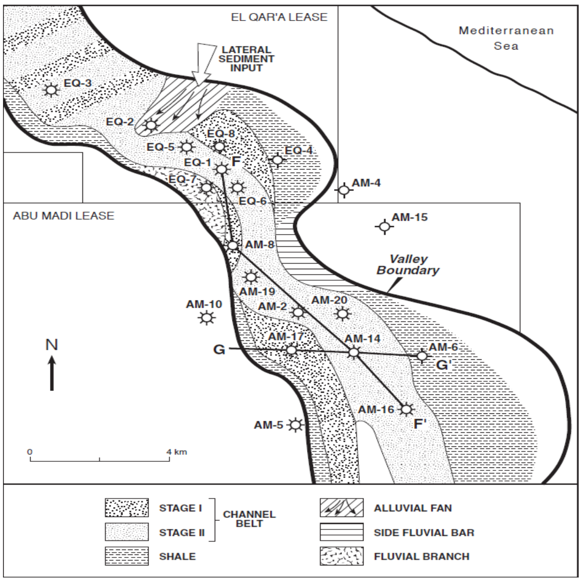

Fig. 2: Depth-structure map of the AB-EQ Field at the level of the Level III reservoir **(Shash *et al*., 1996).**

2. Data set

This study is based on 3D seismic surveys which cover totally the extension of Abu Madi onshore reservoirs. It was acquired by Western Geco group in 2007, using a dynamite energy source. The receiver lines spacing was 300 m apart and the shooting was Brick giving nominal fold and bin size=25x25. Well logs and production data from Level III from the adjacent area used for petrophysical parameters and production data.

2.1. Abu Madi Geological setting

The Abu Madi (AM) Fm. has the lithotype in the AM-1 well, where it attains a thickness of 322 m., **(Rizzini *et al*., 1978)**. This formation is composed of thick sand layers, scarcely conglomeratic, with shale layers interbeds that become thicker and more frequent in the upper part of the formation, **(Alfy *et al*., 1992)**.

AM Fm. (Late Messinian age) is considered the sedimentary infilling of a fluvial paleo valley developed in the subsurface from South (East Delta Concession) to North (Baltim fields) for almost 130 km and from East to West for almost 5 km., **(Dalla, *et al*. 1997)**. AM Fm. has a thickness of about 300 m on average and is characterized by stacked fluvio-deltaic sandstones and shales onlapping content ward (southward) and to the valley flanks against the basal erosional unconformity surface cutting the Qawasim and Sidi Salim Fms. The erosional shape of the Abu Madi paleo valley is due to a dramatic relative lowering of the sea level that occurred in the Late Messinian, **(Palmieri *et al*., 1996; Dalla *et al*., 1997, Dolson *et al*., 2002)**.

The classical Abu Madi Fm. lithostratigraphic section is represented in AM/EQ fields Fig. (3) where the reservoir sandstone levels have been named, starting from the bottom, as follows: Level I, Level II, Level III-A, and Level III.

Fig. 3: Stratigraphic Column and Reservoir Zonation of AM/EQ Fields **(El Heiny *et al*., 1990).**

3. Methods

In this study, we need to estimate the geometry of the reservoir, continuity of sand bodies, and pertophysical parameters. So, structural interpretation, amplitude extraction. Post stack inversion will be carried out to estimate the acoustic properties of the reservoir. P-impedance, petrophysical data, and production history of the wells were used to estimate the presence of reaming gas potentiality.

3.1. Seismic interpretation and Amplitude extraction

Regional horizons interpretation, amplitude extraction, and depth conversion for Abu Madi channel, Level III was derived using Landmark integrated software Fig. (4&5). Well names have been changed to keep the data private.

AM-EQ Field contains two separate sand levels (Levels II and III) Fig. (4) in combination structural-stratigraphic traps within the Upper Miocene Abu Madi Formation. Both reservoirs were deposited within an NW-trending paleo-valley Fig. (5).

Fig.(6) shows Level III trends NW-SE, measures around 22 km long by 1.7-5.8 km wide to the west and east, the top-reservoir terminate abruptly, suggesting the presence of a channel overbank seal.

Amplitude extraction on full volume Fig. (6) shows separate amplitude anomalies that most likely indicate separate sand bodies. Through El Qaraa field, Level III bifurcated into three major fairways, two of them are not yet penetrated by any wells.

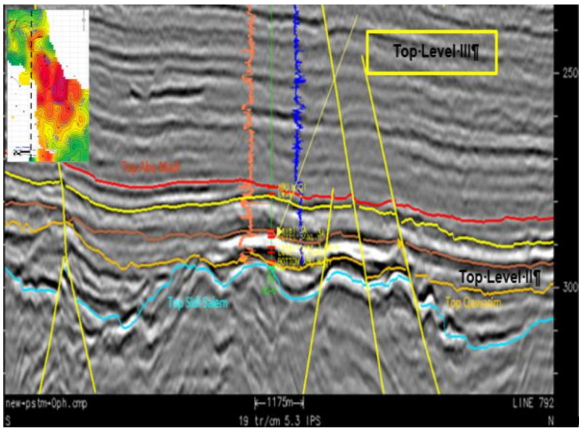

Fig. 4: N-S interpreted cross-section through the northern part of the EQ Field.

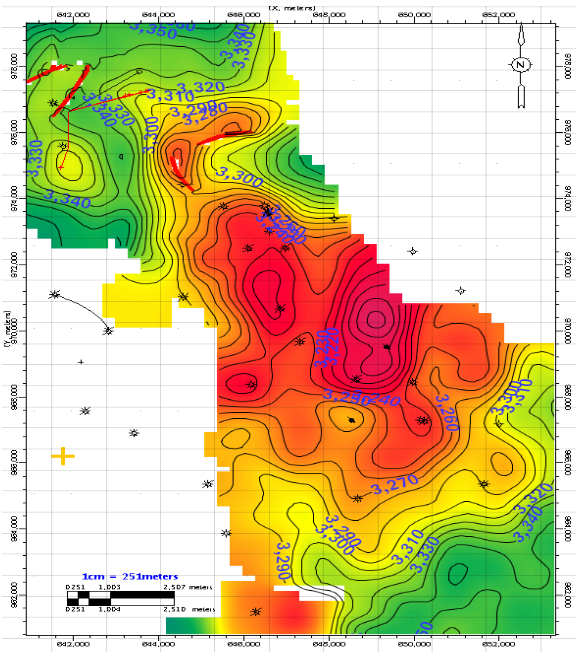

Fig. 5: Depth-structure map of the AB-EQ Field at the level of the Level III reservoir

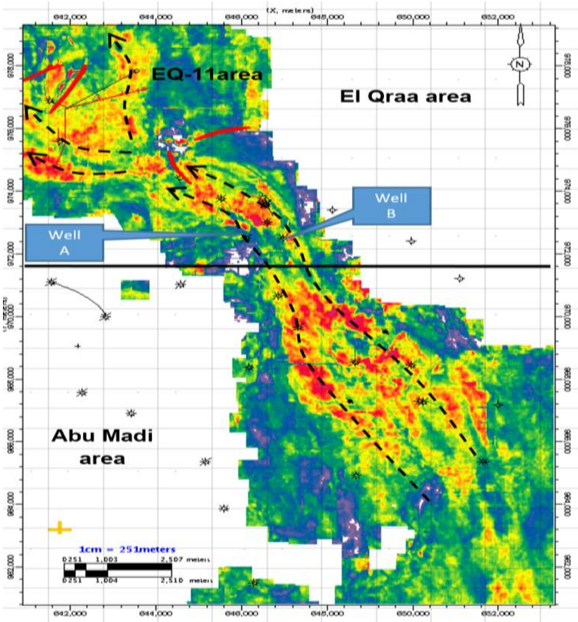

Fig. 6: RMS amplitude map on full-stack at top Level III reservoir in Abo Madi-El Qaraa Field.

Seismic inversion

Inversion of the seismic trace is a technique, which transfers seismic trace data to rock physical properties. Pre-stack and post-stack inversion are two methods of seismic inversion that we can use to analyze inversion results.

Seismic Inversion is the analysis of seismic data using forward modeling Fig. (7).

The forward modeling starts with the bulk density (ρ) and sonic velocity (V) obtained from the well logs, which can generate the reflection coefficient. Reflection coefficient is the ratio of reflected amplitude and incident amplitude:

$$reflection\ coefficient = (V1\rho1 - V2\rho2) / (V1\rho1 + V2\rho2) \qquad \textbf{eq. (1)}$$

Post-stack inversion

The seismic traces in the stacked seismic section could be modeled as the convolution of the earth's reflectivity and a band-limited seismic wavelet. In a post-stack inversion, we assume that seismic traces are zero offsets. It means that they hit the interface and reflect with zero angles. So, The Zoeppritz equations will simplify to the more manageable equation given by Eq. (2).

$$r_i = (Z_{i+1} - Z_i) / (Z_{i+1} + Z_i) \qquad \textbf{eq. (2)}$$

Where r_i is the zero offset reflection coefficient at the i^{th} interface and $Z_i = \rho_i V_i$ is the impedance of i^{th} layer. ρ is density and V_i is P-wave velocity.

Model-based inversion is based on the convolution model. If the noise is uncorrelated with the seismic signal, we can solve the reflectivity satisfying this equation. This is a non-linear and band-limited equation, which can be solved iteratively due to **(Swisi *et al.*, 2009 & Russell *et al.*, 2007)**. That solution is gradually improving the fit between synthetic traces and the observed seismic data. The solution attempts to simultaneously solve the best-fit reflectivity and minimize the differences between the observed and predicted seismic by **Lee *et al*., 2013**.

Since the Seismic data is band-limited, Model-Based inversion gives the advantage of using well data where it contains both low and high-frequency data that are missed in the seismic data.
The model-based method also allows incorporating into the seismic interpretation a model, based on the known or suspected geology. This can result in better resolvability and a link between the seismic data and the lithology.
Before performing seismic inversion VP, VS and P-impedance obtained using well logs. VP-VS ratio versus P-impedance cross plots from the EQ-10 well logs shows that the sandstone reservoirs characterized by low values of VP-VS ratio and high P-impedance Fig. (8 & 9).

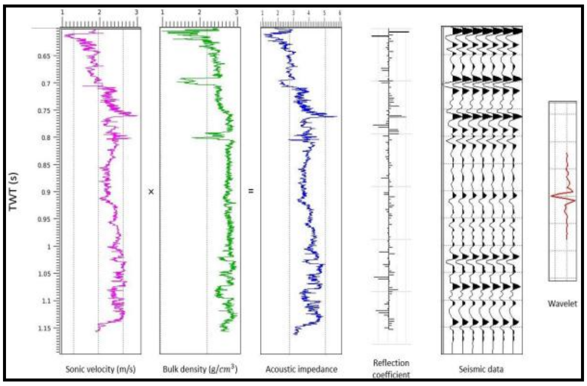

Fig. 7: Forward modeling, after **Wu *et al*., 2015**.

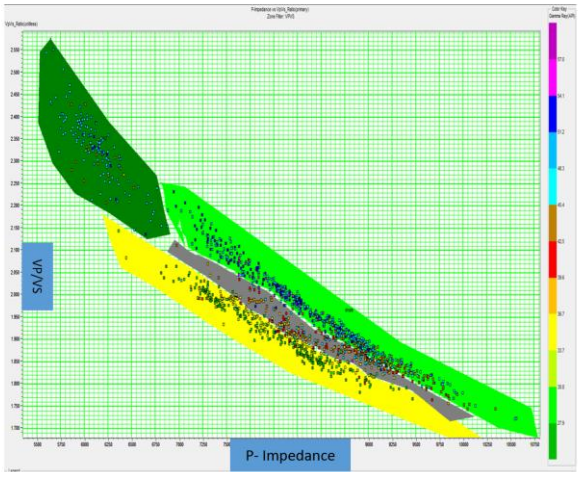

Fig. 8: VP/VS versus P-impedance cross plots and Zonation from the well logs.

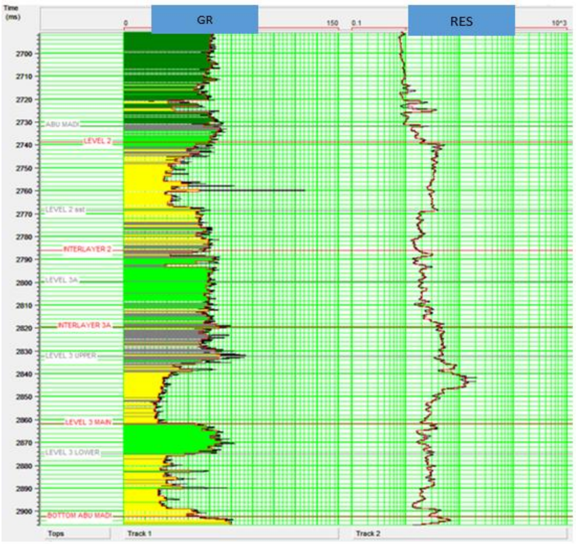

Fig. 9: Zonation of different lithology using VP/VS versus P-impedance cross plots, the left sidetrack shows the gamma-ray plot (GR) while the right side track shows the resistivity plot (RES).

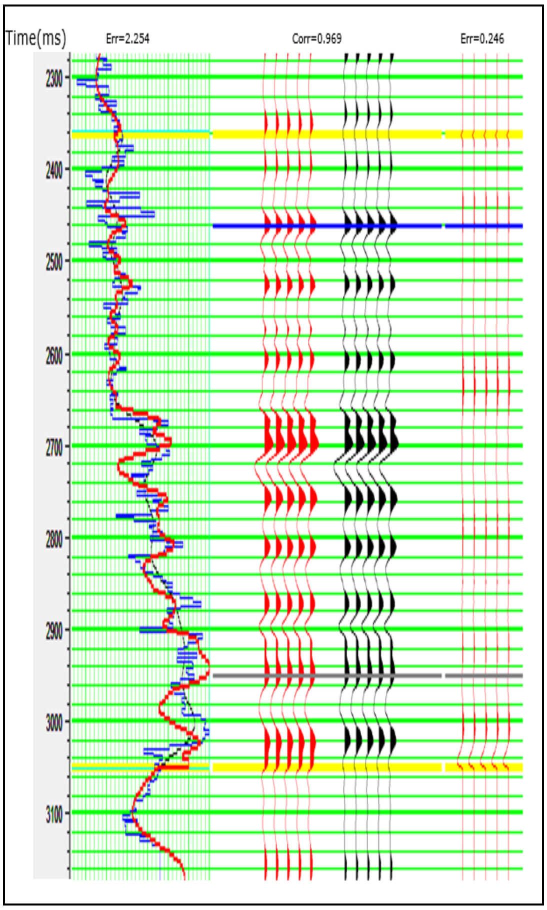

Fig. 10: Low-frequency model QC

To have a VP-VS ratio and P-impedance from post-stack seismic data, model-based inversion had been done. The workflow of the model-based inversion technique is as follows:

- Calculate the Zp and Zs at wells locations using the well log data.
- Pick horizons in the seismic section to control the interpolation and to provide structural information for the model between the wells in the area Fig. (4 & 5).
- Use interpolated seismic horizons and between all wells locations to obtain the initial low-frequency model.

Once the model is built and QC performed Fig. (10), the post-stack data is inverted using Hampson Russell Software.

The outputs of inversion are P-impedance Fig. (11&12) and VP/VS Fig. (13).

Fig. (11) showed low impedance trend looks like the same form amplitude extraction Fig. (6) oriented NNE-SSW, the presences of low impedance areas along the central part of the channel which have high hydrocarbon saturation and also contains producer wells as shown on the map and have a good stratigraphic trap. In addition, there are areas to the southwest end to the east of the channel, with low impedance that, could contain un-produced gas.

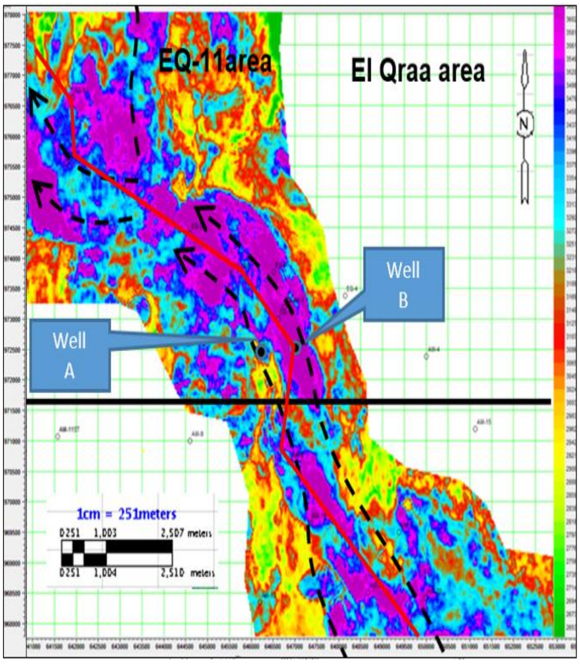

Fig. 11: P-impedance time slice on Level-3 (30 ms centered) window

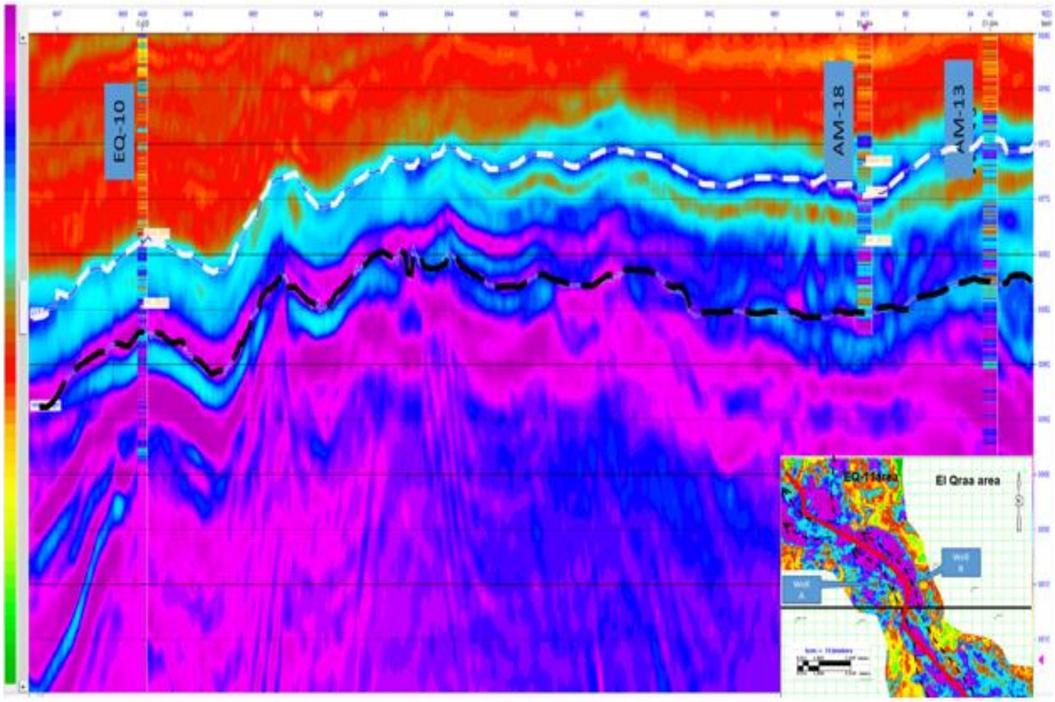

Fig. 12: arbitrary cross-section in Post-stack model-based inverted result P-impedance passing through AM-EQ fields the black dashed line is top Level-lll.-

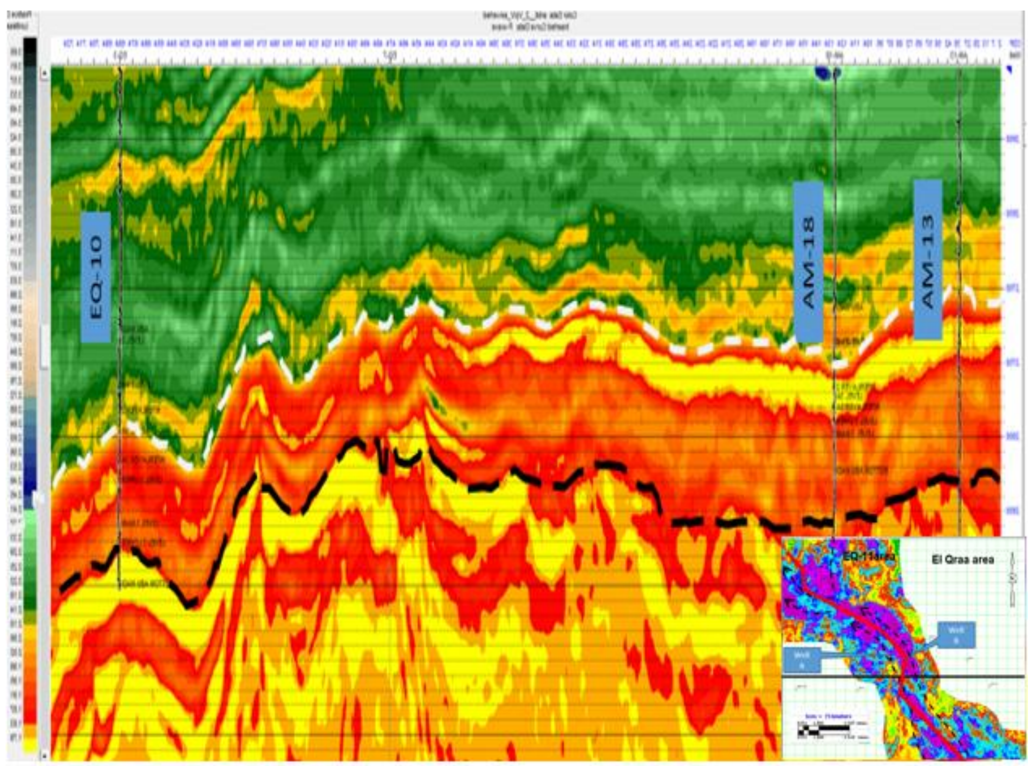

Fig. 13: arbitrary cross-section in Post-stack model-based inverted result VPVS passing through AM-EQ fields the black dashed line is top Level-lll

3.2.Wells history and production data analysis

In this part, we focused on El Qaraa field where we found that at the western part of El Qaraa field 1986, the electric logs of well-A which drilled in 1992 showed the gas down to (GDT) at -3338m although it is in high position than well-B which drilled in 1991 recorded shallower gas-water contact (GWC) at -3333m Fig. (14). From the amplitude and P-Impedance maps the two wells are located in two different channels Fig. (6 &11).

On the other hand, at the northern part of the field, EQ-09, EQ-10, and EQ-11 Fig. (15) wells were drilled in 1986, 1987, and 2010 respectively. From electric logs, we can estimate GWC in the three wells at -3350 for EQ-09, -3361 for EQ-10, and -3327 for EQ-11. IN 1994 the area at EQ-10 well was considered to be exhausted 1994 but in 2010 EQ-11well recorded the presence of gas.

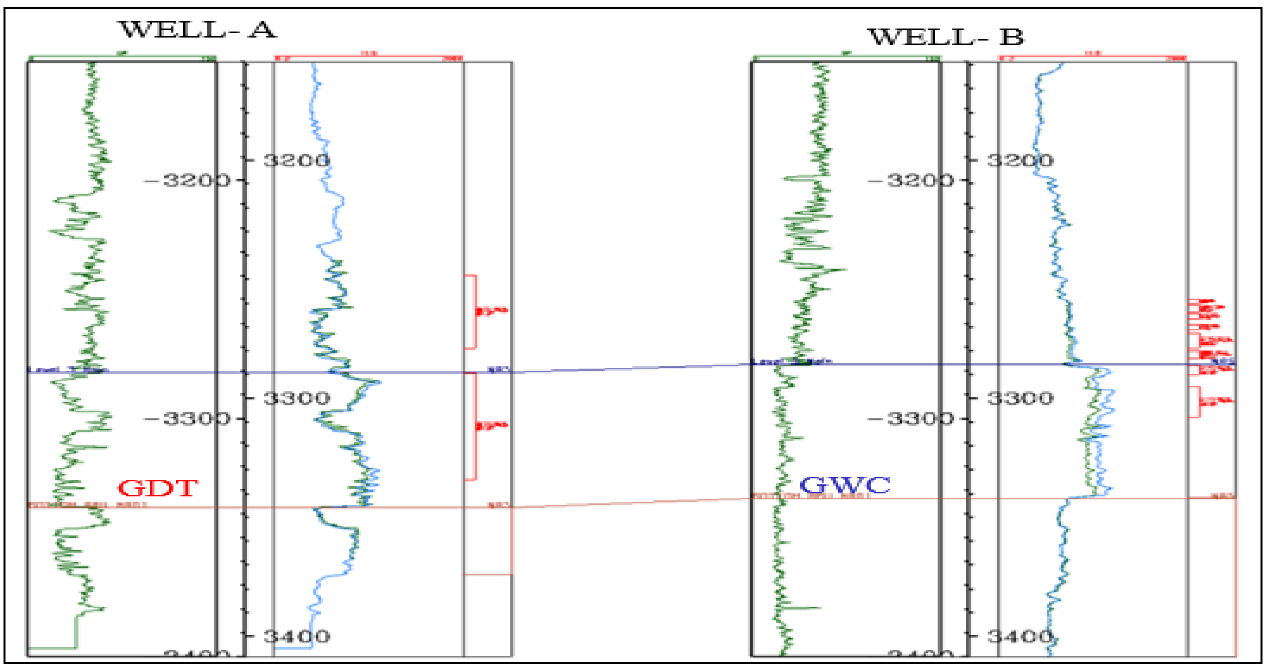

Fig.14: Correlation between Well-A & B shows the perforated interval &water level, the left side track shows the gamma-ray plot while the right side track shows the resistivity plot.

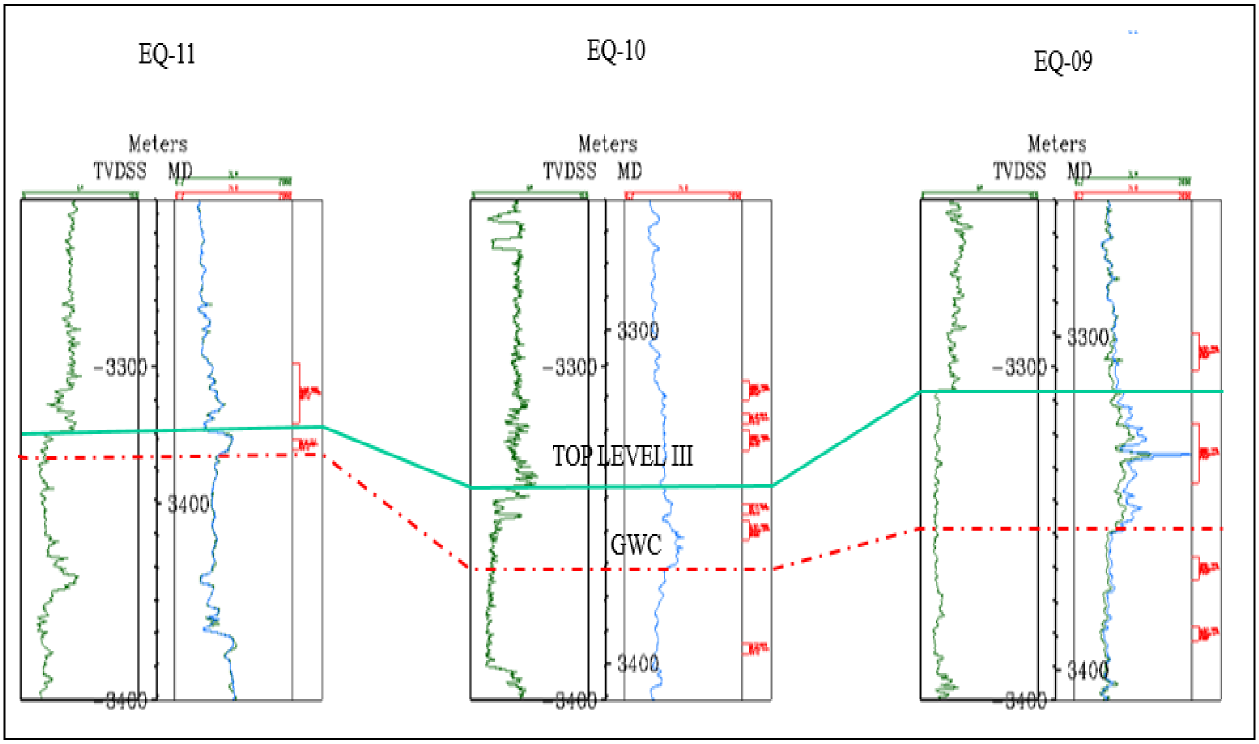

Fig. 15: Correlation shows the difference in GWC, the left side track shows the gamma-ray plot while the right side track shows the resistivity plot.

4. Results and conclusion

The amplitude and P-Impedance maps confirm and give a high-resolution image for Level III where it is represented by a large multi-channel fill sand bodies extended generally in NW-SE direction and bifurcated into three loops in EQ-11 area. The main channel is up to 22 km long and up to 6 km wide Fig. (6).

Interpretation of data from both amplitude and P-Impedance maps showing the area of El Qaraa is stratigraphically separate from the southern Abo Madi area, also the presence of stratigraphically separate sand bodies in the east and west of EQ-11. This answers the presence of different GWC and initial pressure in EQ-11 and the other wells and open rooms for more gas potentials still unrevealed.

P-impedance map Fig. (13) not only shows the extension of sand bodies and heterogeneity of the reservoir but also shows the stratigraphic barriers between sand bodies. This answers the presence of different GWC and initial pressure in EQ-11 and the other wells and supports the idea of the presence of other rooms for more gas potentials still unrevealed.

The production history of Level III shows variation in the G.W.C, also the new interpreted depth amplitude map shows that these anomalies are stratigraphically and structurally separate Fig. (14 & 15).

By integrating the new interpreted structure depth amplitude map with the production data from current and closed wells we found possibilities for the presence of remaining gas potential in the north part of the Level III channel Fig. (16).

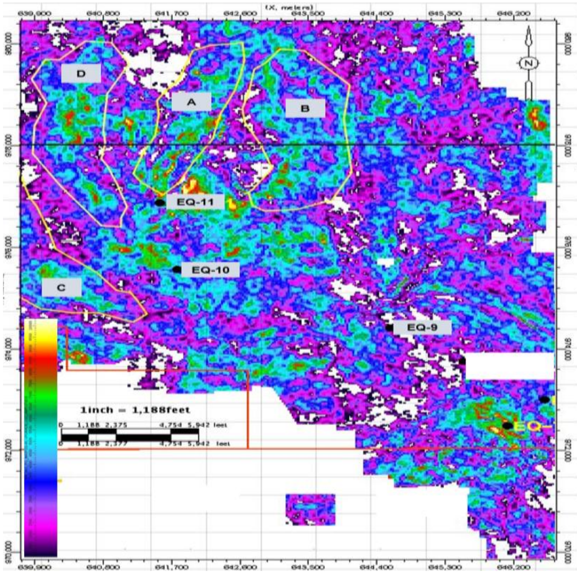

Fig.16: Amplitude map of El Qaraa north area shows the possible gas residual locations (A, B, C & D)

5. REFERENCES

Alfy, M., F. Polo and M. Shash 1992.The geology of Abu Madi gas field. Proceedings of the 11th Petroleum Exploration and Production Conference, Cairo, 1992.

Barbieri, M., Spotti, G., Zaki, M., and Anwar, A., 1992, Abu Madi - El Qar'a Field, Nile Delta, Egypt: reservoir description through cluster analysis methodology - a case study, Proceedings 11th Petroleum Exploration &Production Conference, Production: EGPC, Cairo, p. 639-746.

Dalla, S., H. Harby, and M. Serazzi, 1997, Hydrocarbon exploration in a complex incised valley fill: an example from the late Messinian Abu Madi Formation (Nile Delta basin, Egypt): The Leading Edge, 16: 1819-1824.

Dolson, J.C., Martinsen, R.S. & Sisi, Z.E. 2002c. Messinian incised-valley systems in the Mediterranean along the Egyptian coastline: paleogeography and internal fill:

evidence from cores and seismic (abs.). American Association of Petroleum Geologists International Petroleum Conference and Exhibition. A25.

EGPC, 1994, Nile Delta & North Sinai: fields, discoveries and hydrocarbon potentials (a comprehensive overview: The Egyptian General Petroleum Corporation, Cairo, 387 p.

El-Heiny, I., Rizk, R., and Hassan, M., 1990, Sedimentological model for Abu Madi reservoir sands, Abu Madi Field, Nile Delta, Egypt, Proceedings 10th Petroleum Exploration & Production Conference: EGPC, Cairo, p.1-37.

Lee, K., Yoo, D. G., McMechan, G. A., Hwang, N., Lee, G. H. 2013, Terr. Atmos. Ocean. Sci., 24(3): 295.

Matresu, J., Talaat, A., El BelasyA. M., El-Meadawy, M., 2013, Pre-Messinian Extensional Tectonics and exploration potential of related structures; in Central Nile Delta Basin, Egypt; North Africa Technical Conference and Exhibition, 15-17 April, Cairo, Egypt

Palmieri, G., Harby, H., Marini, J.A., Hashem, F., Dalla, S. & Shash, M. 1996. Baltimfields complex: an outstanding example of hydrocarbon accumulations in a fluvial Messinian incised valley. In: Proceedings of the 13th Petroleum Conference, Cairo, Egypt Reservoir 3D Compositional Model Study, 1988, –Lev II & Lev III- Abu Madi-El Qara field.

Reservoir Evaluation Report, 2002, Abu Madi –El Qa'ra Field-Northen Nile Delta, Egypt.

Rizzini, A.; Vezzani, F.; Cococcetta, V. and Milad, G; 1978, Stratigraphy and sedimentation of Neogene-Qaternary section in the Nile Delta area. - Marine Geology 27: 327-348.

Russell, H., "STRATA guide," Hampson-Russell, CGG Veritas, (2007).

Said, R. (1962), The Geology of Egypt. Elsevier Publishing Co., New York, 259.

Salem. M; 1976, Evolution of the Eocene-Miocene sedimentation pattern in northern Egypt. - AAPG-Bull. 60:34-64.

Shash, M., Rizk, R., and Zaki, M., 1996, Depositional model and its impact on the water breakthrough in Abu Madi El Qar'a gas field, Nile Delta, Egypt, Proceedings 13th Petroleum Exploration & Production Conference, Exploration, v. 2: EGPC, Cairo, p. 285-311.

Swisi, A., "Post- and Pre-stack Attribute Analysis and Inversion of Blackfoot 3D Seismic Data Set," M. Sc. Thesis, Geological Sciences, University of Saskatchewan, Saskatoon, 2009.

Zoeppritz, K. 1919, On the reflection and propagation of seismic waves. Erdbebenwellen VIIB, Gottinger Nachrichten I, pp. 66-84.

تكامل الخصائص الزلزالية ثلاثية الأبعاد وتاريخ الإنتاج في إعادة تقييم إمكانات الغاز في حقلي أبو ماضي والقرعة

أ.د. عادل عثمان[١]، أ.د. محمد فتحي[١]، د. جاستن ماتريشيو[٢]، محمد نصار.[٣]

[١] **جامعة الازهر، مدينة نصر، القاهرة، مصر.**
[٢] **شركة إيني الدولية.**
[٣] **شركة بترول بلاعيم (بتروبل) ، مدينة نصر، القاهرة، مصر.**

يعد استخدام البيانات السيزمية مثل سمات التغير في السعة مع الازاحة وطرق الانعكاس طرق فعالة في التنبؤ بخصائص المكامن الهيدروكربونية ، خاصة في الخزانات غير المتجانسه كما في حقول الغاز في منطقة دلتا النيل. التحدي الرئيسي في منطقة الدراسة الحالية ممثلة في حقلي ابو ماضي و القرعة هو أن معظم الآبار المحفورة في المنطقة إما مستنفدة أو امتلئت بالماء. لذا فإن تحديد الخزانات الرملية الحاملة للغاز باستخدام الأساليب الزلزالية التقليدية فقط سيكون موضع تساؤل.

تتميز الحقول القديمة بتوفر الكثير من البيانات الفيزيائية وبيانات الإنتاج. تساعد البيانات الفيزيائية والبتروفيزيائية وتاريخ الإنتاج على فهم خصائص الخزان مثل المسامية والكثافة ومحتوى السوائل والحد الفاصل بين الغازوالماء.

ركزت هذه الدراسة على استخدام ودمج نتائج البيانات البتروفيزيائية والإنتاجية مع نتيجة الانعكاس الزلزالي لتحديد توزيع خزان الرمل الغازي وخصائص المكمن.

لتحقيق الهدف من الدراسة تم إنشاء الخرائط التركيبية وخرائط السعة وخرائط المعاوقة الصوتية لتوضيح الصورة لمستويات الخزان الرملي لمكمن أبو ماضي. تم مراجعة تاريخ إنتاج آبار الإنتاج الحالية والمغلقة ودمجها مع النتائج الزلزالية. بناءا على نتائج هذه الدراسة تم تحديد بعض مناطق الغاز المتبقية المحتملة في حقلي ابو ماضي والقرعة.